

Synthesis of EVA-g-PLA copolymers using transesterification reactions

I. Moura ^{a,*}, R. Nogueira ^b, Véronique Bounor-Legare ^c, A.V. Machado ^a

^a Institute of Polymers and Composites/I3N, University of Minho, 4800-058 Guimarães, Portugal

^b Institute for Biotechnology and Bioengineering, Centre of Biological Engineering, University of Minho, 4705-057 Braga, Portugal

^c University of Lyon, CNRS UMR5223, IMP@Lyon1, 15 Boulevard Latarjet, 69622 Villeurbanne, France

Keywords:

Ethylene vinyl acetate
Polylactide
Transesterification
Grafting
Biodegradable

Abstract

The synthesis of EVA-g-PLA grafted copolymers was carried out by reactive extrusion, through transesterification reaction between ethylene vinyl acetate copolymer (EVA) and polylactide (PLA), using titanium propoxide ($\text{Ti}(\text{OPr})_4$) and titanium phenoxide ($\text{Ti}(\text{OPh})_4$) as catalysts. Different materials were prepared by changing the relative amount of polylactide and catalyst. The extent of the grafting reaction, which depends on the quantity of polylactide and catalysts, was estimated by selective extractions. The influence of the same parameters on the final structure, morphology and thermal and mechanical properties was also evaluated. The results showed that $\text{Ti}(\text{OPr})_4$ exhibited higher efficiency as a catalyst than $\text{Ti}(\text{OPh})_4$. Moreover, using the former catalyst, 25wt.% of EVA-g-PLA copolymer was synthesized. The sample containing the higher amount of copolymer exhibits the better properties and the higher biodegradability.

Introduction

The rapid growth of plastic production is considered as a serious source of environment pollution. Approximately 100 million tons of plastics are produced each year and within a short period of time almost half of them are disposed to the environment [1]. A way to overcome this problem would be the use of biodegradable polymers. However, this has not yet proven to be useful for commercial applications due to their high price or limitations in terms of thermal and mechanical properties [2].

In the recent years, a lot of effort has been made to develop lowcost and environmentally friendly materials through blending and modification of biodegradable polymers [3,4]. The use of blends or copolymers of biodegradable and non-biodegradable polymers called bio-based polymers, could be an alternative to conventional non-biodegradable plastics and contribute to the solution of the environmental problem. Even though these polymers are not completely biodegradable, they have economic advantages and better properties than biodegradable ones.

Blends of natural and synthetic biodegradable polymers, such has, starch, poly(ϵ -caprolactone) and polylactide and nonbiodegradable synthetic polymers, for example, polyolefins,

polystyrene and ethylene vinyl acetate have been widely studied for a variety of industrial applications [5,6].

Since polyolefins present a combination of physical properties that are ideally suited to a wide variety of applications, many studies have been carried out blending them with biodegradable polymers [5,7-9]. Contat-Rodrigo and Greus [8] and Matzinos et al. [9] blended polyethylene (PE) and biodegradable polymers (polylactide (PLA) and poly(ϵ -caprolactone) (PCL)) to increase the mechanical properties. Matzinos et al. [9] found out that the mechanical properties of the blends depend not only on its content but also on the final morphology. Machado et al. [5] investigated the mechanical properties and biodeterioration of blends of high density polyethylene (HDPE) and poly (ϵ -caprolactone), polylactide and starch. It was observed that while the blend containing PLA had higher Young's modulus and lower elongation at break than HDPE, the blend containing PCL had the opposite behavior. The biodeterioration was higher for blends containing PCL.

Since the morphology of the blends has a major effect on mechanical properties, another approach to prepare bio-based polymers is by synthesis of copolymers of non-biodegradable synthetic polymers and biodegradable ones [10]. Within one copolymer different repetitive units can be present and can be either distributed statistically along the polymer chains (random copolymers), alternately, form a block (block copolymers) or a branching structure (grafted copolymers). These different structures, despite having the same overall composition, can have different properties. Moreover, copolymers have been developed to generate new materials with enhanced performance. The interest of these materials is linked to the in situ compatibilization of

Table
Composition of the prepared samples.

Sample	EVA (wt. %)	PLA (wt. %)	Ti(OPr) ₄ or Ti(OPh) ₄ (wt. %)
--------	-------------	-------------	--

EVAPLA0	60.0	40.0	0.0
EVAPLA1	59.5	40.0	0.5
EVAPLA2	59.5	39.8	0.7
EVAPLA3	59.5	39.6	0.9
EVAPLA4	59.5	38.6	1.9

polymer blends [11], where the grafted copolymer formed during blending reduces the surface tension, prevents droplets coalescence and consequently generates polymer blends with enhanced properties.

Moura et al. [12], synthesized copolymers of EVA-g-PLA and EVA-g-PCL through in situ polymerisation of lactide and/or ϵ -caprolactone in presence of EVA using titanium phenoxide ($\text{Ti}(\text{OPh})_4$) as catalyst. The obtained materials exhibited better mechanical properties and higher biodegradability than the correspondent blends of EVA and PLA or EVA and PCL.

The present work aims to prepare copolymers of EVA-g-PLA through transesterification reactions between ethylene vinyl acetate (EVA) and polylactide (PLA) catalysed by $\text{Ti}(\text{OPh})_4$ and $\text{Ti}(\text{OPr})_4$. The effect of the amount of grafted copolymer (EVA-g-PLA) on biodegradability, mechanical properties and other physical properties was investigated.

Experimental

Materials

Ethylene vinyl acetate copolymer (Escorene Ultra Lot. 61E466) with 28wt.% of vinyl acetate ($M_n = 18,000 \text{ g mol}^{-1}$), supplied from Exxon was used as a non-biodegradable synthetic polymer and polylactide (PLA) ($M_n = 22,000 \text{ g mol}^{-1}$) supplied by Sigma Aldrich was used as a biodegradable polyester. Titanium propoxide ($\text{Ti}(\text{OPr})_4$) from Aldrich and titanium phenoxide ($\text{Ti}(\text{OPh})_4$), prepared according to a procedure published elsewhere [13], were used as a transesterification catalysts.

Synthesis of EVA-g-PLA graft copolymers

The composition of the prepared samples is shown in Table 1. The pellets of both polymers were dried in a vacuum oven at 60°C for 24 h before use. Samples were prepared in a Haake batch mixer (Rheocord 90; volume 50 ml), equipped with two rotors running in a counter-rotating way. The rotor speed was 50 rpm and the set temperature was 160°C . The copolymers were prepared using the following sequence: first EVA pellets were introduced into the hot mixer, after melting, PLA and the catalyst were added. Both catalysts were collected and carried to the mixer under argon atmosphere, to prevent hydrolysis reaction. After 20 min the rotors were stopped and the total sample was removed.

Samples for XRD, rheology and mechanical properties were prepared by compression moulding in a hot press at 160°C during 5 min under a pressure of 10 tons.

Copolymer identification and characterization

The synthesized graft copolymers, EVA-g-PLA, were characterized by several analytical techniques described below.

Extraction of copolymer

The EVA-g-PLA copolymers produced by reactive extrusion were isolated from the other components according to the method previously described in Moura et al. [12] and summarized in Fig. 1.

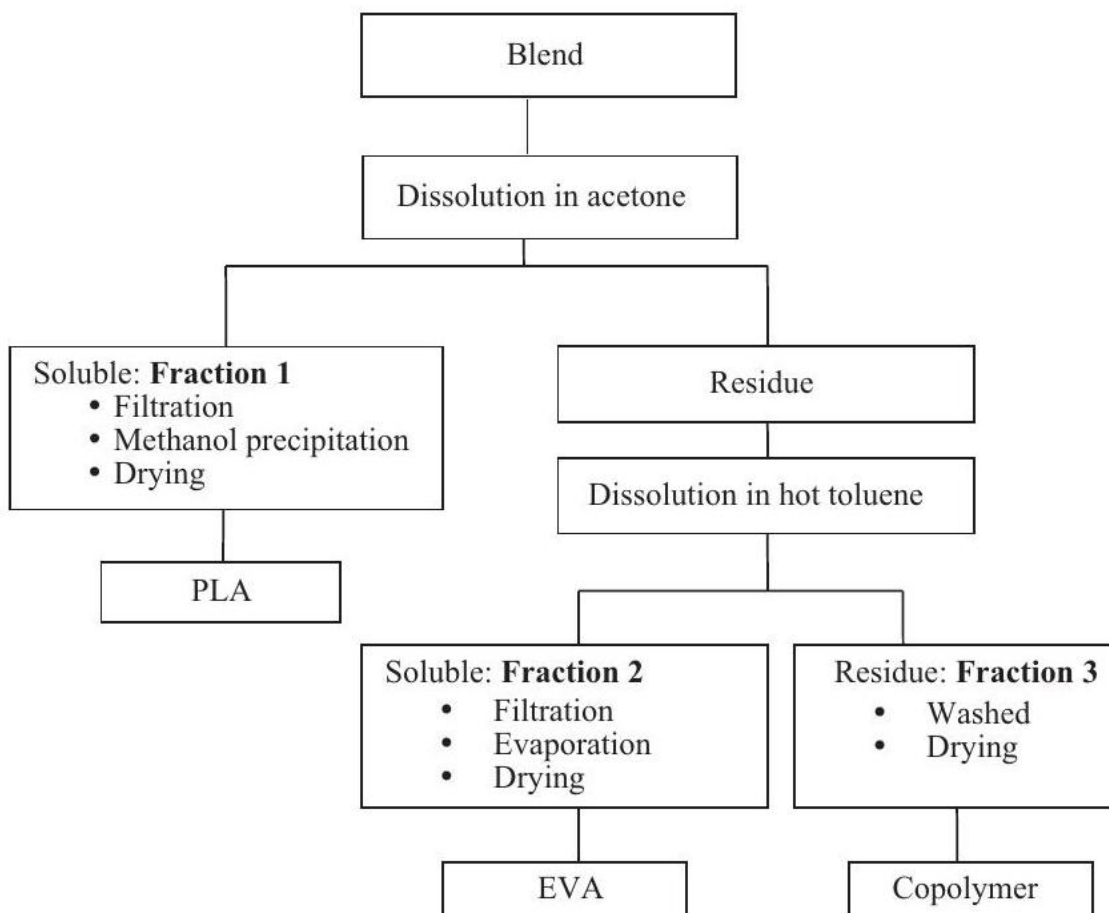


Fig. 1. Scheme of polymers and EVA-g-PLA copolymers extraction.

Structural characterization

2.3.2.1. ^1H NMR. High resolution liquid ^1H NMR spectroscopy was carried out with a Varian 343 K instrument at 300 MHz for ^1H . Deuterated chloroform, CDCl_3 was used as a solvent for analysis. Chemical shifts (δ) are in ppm with reference to internal tetramethylsilane (TMS).

2.3.2.2. X-ray diffractometry (XRD). Initial polymers and all prepared samples (EVAPLA0 to EVAPLA4) were subjected to XRD analysis. The X-ray diffractograms were performed in an automatic diffractometer, Philips Analytical X-ray PW 1710 BASED, using $k\alpha$

radiation of a copper ampoule ($I = 1.54056 \text{ \AA}$), operating at a cathode current of about 30 mA and a voltage around 40 kV. The diffractograms were performed between 0° and $60^\circ(2\theta)$ with a scanning speed of $2\theta \text{ min}^{-1}$. The standard calibration was made using a silicon standard. Films of the samples were placed in an aluminium sample holder.

2.3.2.3. Rheological properties. Oscillatory rheological measurements of original polymers and produced samples were carried out in an AR-G2 rotational rheometer at 160°C using a parallelplate geometry. The gap and diameter of the plates were 1 mm and 4.0 cm, respectively. A frequency sweep from 0.01 to 100 Hz under constant strain was performed for each sample.

2.3.2.4. TGA and DSC. All samples were analysed using a TGA 2950 thermobalance operating under a nitrogen flow atmosphere (50 mL min^{-1}). Samples were heated from 35 to 600°C at a heating rate of 10°Cmin^{-1} .

Thermal properties of all samples were measured using TA Instruments differential scanning calorimeter (DSC 2920). Samples were heated from 25 to 200°C at a heating rate of 10°Cmin^{-1} , cooled down to room temperature at the same rate, under liquid nitrogen, in order to eliminate the thermal history of the material. Then, they were heated again until 200°C and cooled to room temperature at the same heating rate. The crystallinity degree (X_c) was calculated by ratio of ΔH_f (the apparent melt enthalpy measured from the DSC curves as melting enthalpy per gram) corresponding to the component and ΔH_f^0 (the melt enthalpy per gram of the component in its completely crystalline state).

2.3.2.5. SEC. The number average molar mass (\bar{M}_n) and polydispersity were measured by size exclusion chromatography. Solutions were prepared in chloroform (99.9%) and prefiltered on filter plate (hydrophobic polytetrafluoroethylene, $0.45 \mu\text{m}$ pore size) before injection. The analysis was performed in a SEC Waters 150-CV apparatus equipped with 3 Waters Ultrastaygel columns (HR1 and HR4; inner diameter = 7.8 mm , length = 300 mm and particle size = $5 \mu\text{m}$) and with a viscometer and refractometer detectors. Chloroform was used as eluent with a flow rate of 1 mL min^{-1} and at 23°C . The calibration curve was previously obtained with polystyrene standards with narrow molar mass distribution.

2.3.2.6. SEM. The morphology of the samples was analysed with a FEI Quanta 400 Scanning Electron Microscope (SEM), after fracturing the samples in liquid nitrogen and coating with a gold thin film.

2.3.2.7. Mechanical properties. Mechanical experiments were performed in a ZWICK apparatus using a test speed of 5 mm min^{-1} , EVA $-\text{CH}_2 - \text{CH}_2 - \text{CH} - \text{CH}_2 -$ at room temperature and relative humidity of 50%. The tests were performed on $2.5 \text{ cm} \times 0.8 \text{ cm}$ rectangular samples in a longitudinal direction. At least 6 specimens of each sample were tested. Prior to mechanical measurements, films were prepared by compression moulding using the samples that were removed from the mixer.

2.3.2.8. Biodegradability assessment. Biodegradation tests were carried out in aqueous environment under aerobic conditions according to the standard ISO 14851:1999 (determination of the ultimate aerobic biodegradability of plastic materials in an aqueous medium) [14], which specify a method for determining the biochemical oxygen demand (BOD) in a closed respirometer. This procedure was previously described in Moura et al. [12].

2.3.2.9. FTIR. FTIR spectra of all samples before and after biodegradation were recorded using a Perkin Elmer 1720 spectrometer in the range of $4000 - 500 \text{ cm}^{-1}$, using 16 scans and a resolution of 4 cm^{-1} . Thin films of the initial materials and the residues after biodegradation were prepared by compression moulding and analysed directly using a solid film support.

2.3.2.10. Elemental analysis. The composition of all samples was determined by elemental analysis on a LECO CHNS-932. The amount of carbon, hydrogen and oxygen was determined.

Results and discussion

Structural characterization

Table 1 gives the composition of the prepared samples, amount of polymers (EVA and PLA) and catalyst. The amount of PLA and titanium propoxide/phenoxide was varied in order to investigate

Table 2
Fractions amounts of polymers and copolymers extracted of the samples prepared with $Ti(OPr)_4$.

Sample	Fraction 1 (PLA) (wt.%)	Fraction 2 (EVA) (wt.%)	Fraction 3 (EVA-g-PLA) (wt.%)
EVAPLA0	40.0	60.0	-
EVAPLA1	39.0	59.0	2.0
EVAPLA2	39.0	58.0	3.0
EVAPLA3	37.0	55.0	8.0
EVAPLA4	29.0	46.0	25.0

the effect of catalyst type and amount on the copolymer formation. Therefore, a physical blend (without catalyst) and blends containing four different amount of catalyst were prepared. The expected copolymers were obtained through a transesterification reaction according to the following mechanism [15] and catalysed by the titanium alkoxide derivative:



Since the solubility tests showed that EVA was soluble in hot toluene but insoluble in acetone and PLA was soluble in acetone at room temperature but insoluble in hot toluene, the procedure described in Fig. 1 was followed. Therefore, two grams of each sample were added to 160 mL acetone and stirred at room temperature for 5 days, approximately. Following this, the suspension was filtered. The clear solution was precipitated in methanol and the resulting precipitate was dried until constant weight. This product is referred as fraction 1 (PLA). The insoluble fraction of the first filtration was extracted in hot toluene during 3 days. The solution obtained was filtered, evaporated in a rotational evaporator and dried. The fraction obtained is denoted as fraction 2 (EVA). The residue of this second extraction was washed with methanol, to remove possible existing impurities, and subsequently was dried. This third fraction is the copolymer.

As expected, the amount of each polymer extracted in the physical blend (EVAPLA0) is the same as the amount of polymer used and no copolymer was formed (Table 2). The

amount of copolymer extracted for all the samples prepared using titanium phenoxide as catalyst was nil. This means that no reaction occurred between PLA and EVA esters groups when this catalyst was used. This could be due to the steric hindrance of phenyl groups brought by the titanium phenoxide as already noticed in our previous works dedicated to cyclic ester ring-opening polymerisation catalysed by this titanium derivative [12,13,15].

Table 2 shows the amount of polymers and copolymers extracted for each sample prepared using titanium propoxide as catalyst. Three different fractions were obtained: fractions 1 and 2, corresponding to PLA and EVA and fraction 3 corresponding to the copolymer (EVA-g-PLA) formed during the reaction. All fractions were analysed by ^1H NMR to get information on its composition. As an example, Fig. 2 depicts the spectra obtained for fractions 1 and 2 extracted from EVAPLA4, which confirm that only PLA and EVA are presented. Unfortunately, owing to the insolubility of the EVA-g-PLA copolymer in a series of organic solvents, ^1H NMR analysis

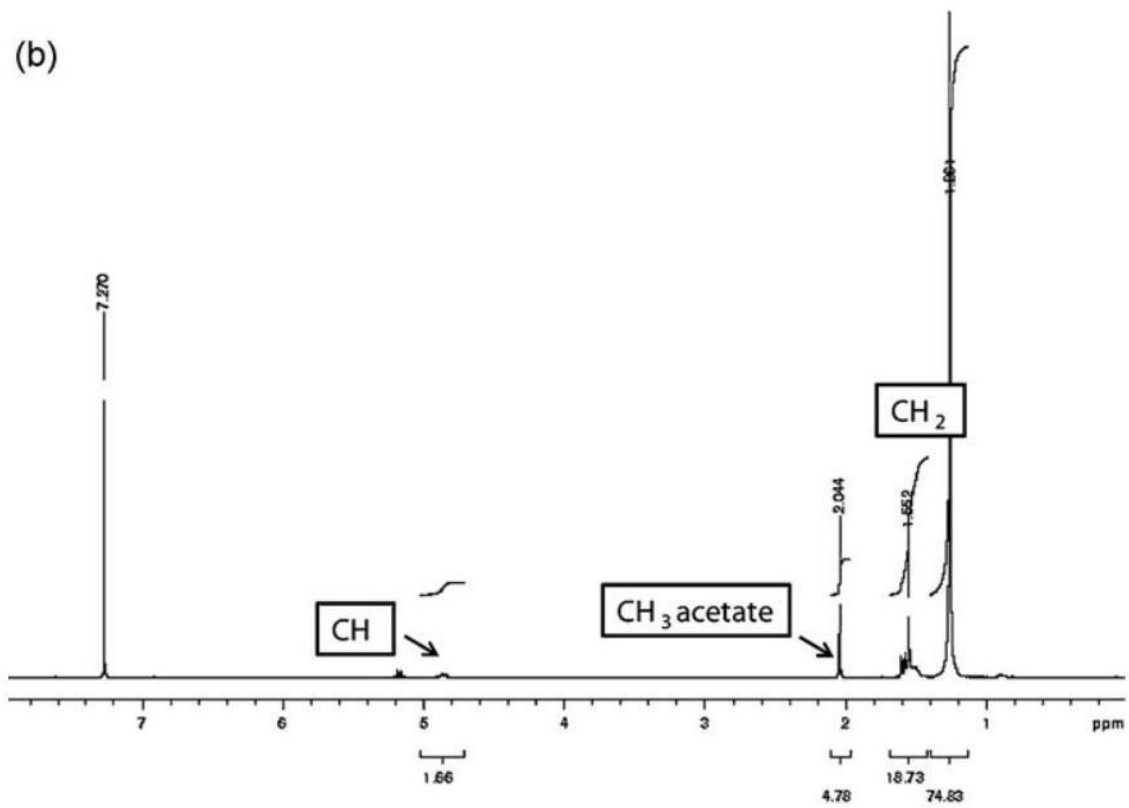
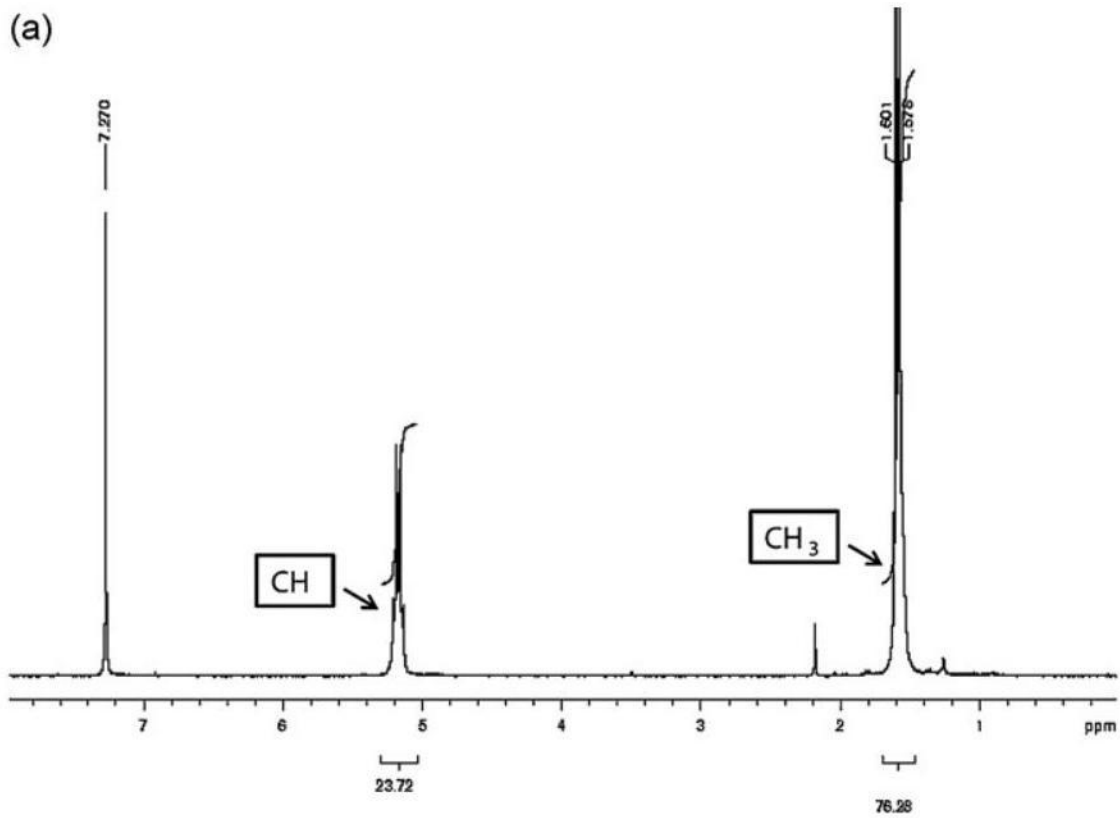


Fig. 2. ^1H NMR spectra of (a) fraction 1 (PLA) and (b) fraction 2 (EVA) extracted from EVAPLA4.

could not be performed. As expected, the highest amount of copolymer, around 25wt%, was obtained for EVAPLA4 with the highest amount of catalyst followed by EVAPLA3, EVAPLA2 and EVAPLA1.

X-ray measurements were performed to analysed structural changes due to copolymer formation. The X-ray diffraction spectra of EVAPLA0 and EVAPLA4 samples are presented in Fig. 3. While EVAPLA0 sample has a sharp diffraction peak at 21.35° , similar to EVA, and a few small peaks around 23.6° , sample EVAPLA4 exhibits

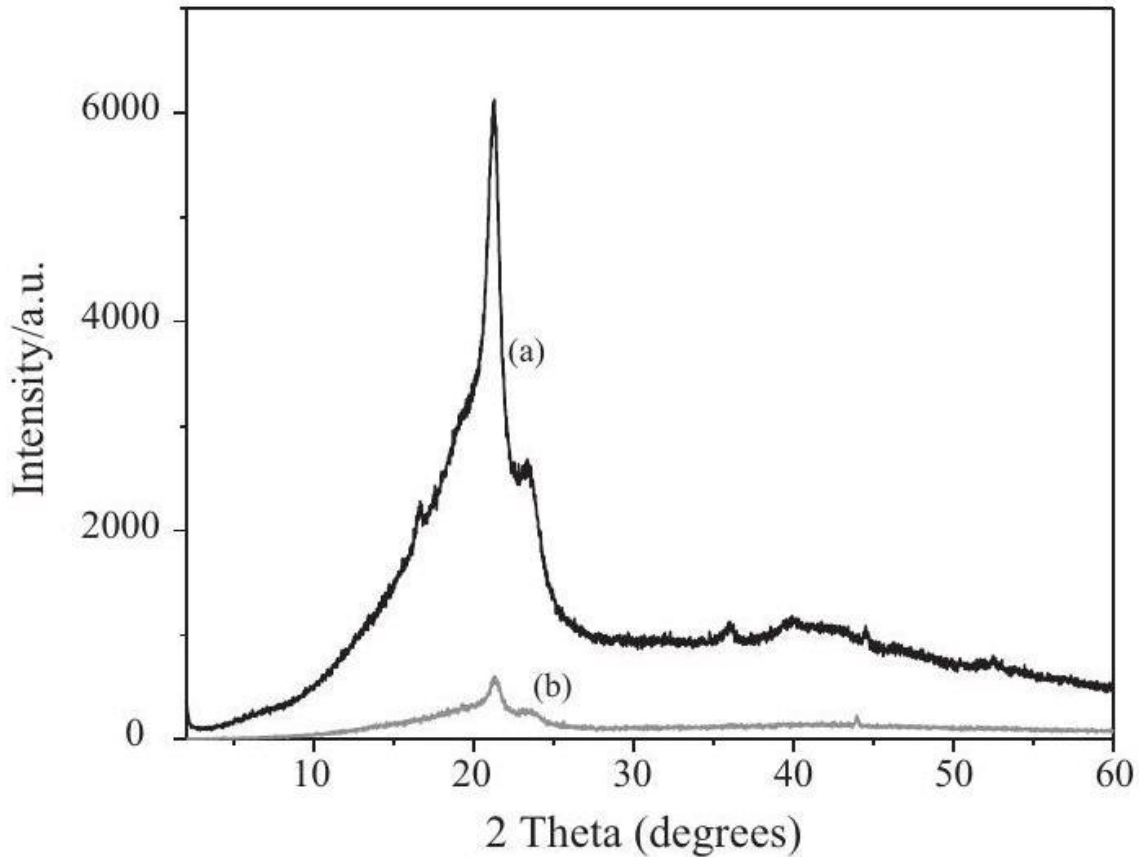


Fig. 3. XRD diffraction patterns of (a) EVAPLA4 and (b) EVAPLA0. the same peaks as EVAPLA0 and a new peak at around 15° . This new peak can be attributed to a different crystalline phase, which can be due to the presence of the copolymer. Moreover, these results indicate that titanium propoxide is not in polymorphous form, but connected to the structure, where it acts as a template (structuring agent) and consequently promotes not only the appearing of the new peak, but also the angle shifts for low values, due the changes occurred in the planar orientation [16].

Oscillatory rheological measurements were carried out to get information on the structure of the copolymer formed. The complex viscosity and storage modulus as a function of frequency are shown in Fig. 4a and b, respectively. Despite all samples showing a non-Newtonian behaviour, differences exist among them. With the exception of the samples

with the highest amount of copolymer (EVAPLA4), the viscosity and the modulus of the other samples are between the curves of PLA and EVA. The sample without catalyst (physical blend), presents, as expected, the lower complex viscosity (1.8×10^4 Pa s) and elastic modulus (7.8×10^2 Pa) at low frequency (0.01 Hz). As the amount of catalyst increases, i.e., the amount of copolymer formed increases, the complex viscosity and elastic modulus at low frequencies shifts to higher values, in agreement with the extractions results. The complex viscosity and the elastic modulus of sample EVAPLA4 is higher than for EVA (7.2×10^4 Pa s and 3.2×10^4 Pa , respectively at $f = 0.01$ Hz). Moreover, the slope of this curve is different from the other samples, which can be associated with a more branched structure of the copolymer formed in this sample. Since this blend has a higher amount of copolymer it is expected that it has higher number of ester groups of EVA linked to PLA chains. Therefore, it will behave as a branched structure, which explains the high complex viscosity and elasticity at low frequencies. These results corroborate that copolymer formation occurred during sample preparation.

Fig. 5 depicts the thermal behaviour of EVA, PLA, and prepared samples when heated from 35°C to 600°C at a heating rate of 10°Cmin⁻¹. In the case of EVA two weight lost steps can be observed. A first one around 300°C (12.44%), attributed to the decomposition of the acetate groups, i.e., release of acetic acid [17]. At approximately 370°C, a second weight lost (86.94%) can be noticed, corresponding to the degradation of the olefinic part of the copolymer (C – C and C – H bonds). PLA presents a one-step decomposition profile with a single decomposition temperature. This polymer has lower thermal stability than EVA, because its degradation peak is around 250°C and it decomposes completely (0% char residue) at 300°C.

All the prepared samples also show two steps degradation, corresponding to the degradation of the individual components. EVAPLA0 sample has an intermediate behaviour between EVA and PLA, being the first decomposition temperature (251.8°C) close to the one of PLA and the second (290°C) close to the one of EVA. Since this sample is a physical blend of EVA and PLA, this behaviour would be expected. Even though, the thermal behaviour of the all other samples is similar to EVAPLA0, a shift to higher decomposition temperatures can be observed, which increases as the amount of catalyst increases. This might be associated with the amount of grafted polymer present in each sample and its branching structure, which seems to contribute to an increase of the thermal stability.

SEC analysis of polymers and all prepared samples were performed to confirm copolymer formation and its effect on molar mass. Table 3 presents the number average molar mass (\bar{M}_n) measured and Fig. 6 depicts chromatograms of the neat polymers (EVA and PLA) and prepared samples. Each initial polymer has a single peak. Even though, the EVAPLA0, EVAPLA1 and EVAPLA2 present only one peak, which can be explained by the similarity of the molar mass of neat polymers (18,000 and 22,000 g mol⁻¹ for EVA and PLA, respectively), some differences can be noticed among them, which can be related to the amount of copolymer present. EVAPLA3

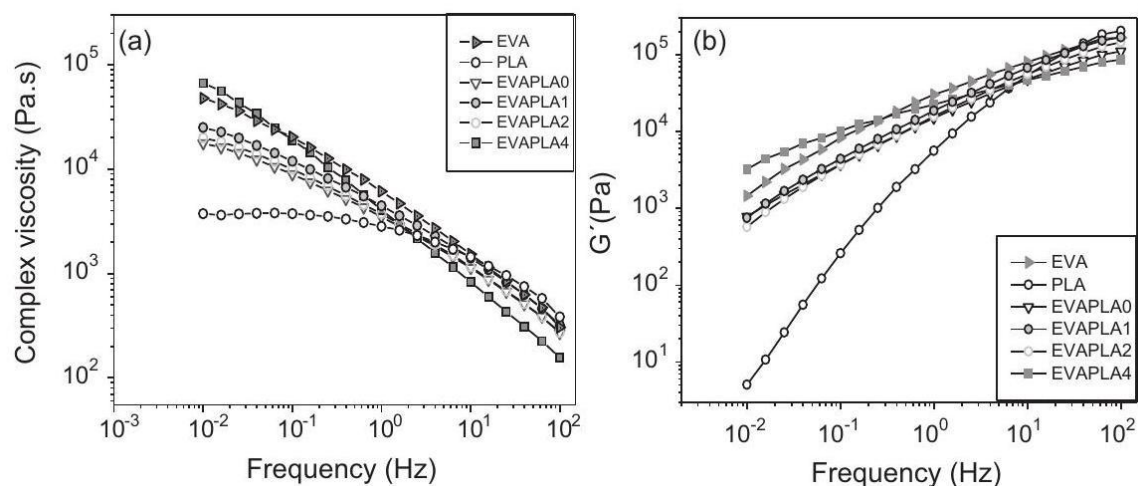


Fig. 4. Rheological behaviour of the individual components and prepared materials (a) complex viscosity and (b) storage modulus.

Table

\bar{M}_n obtained from SEC measurements for neat polymers and prepared samples before and after biodegradation. 3

Sample	\bar{M}_n (from the datasheet)	\bar{M}_n (before degradation)	\bar{M}_n (after degradation)
EVA	18,000	18,831	15,943
PLA	22,000	24,046	3171
EVAPLA0	-	20,122	19,288
EVAPLA1	-	20,235	19,245
EVAPLA2	-	20,741	18,885
EVAPLA3	-	20,814	18,310
EVAPLA4	-	23,900	17,800

and EVAPLA4 exhibit a different behaviour, the chromatograms of both samples have a different shape, two peaks with a retention time of 22.1 and 24.7 min can clearly be noticed in EVAPLA4. This suggests that molecules with different molar mass are presented in this sample. Since 25wt% of copolymer was achieved, both an increase in molar mass and a shift of the chromatogram to lower retention time would be expected but was not observed. A possible explanation is the degradation of PLA in the presence of titanium propoxide during transesterification reaction. Moreover, overlapping this chromatogram with the individual components, it can be detected that this one has a broader elution time than the individual polymers, i.e., it covers higher retention time, which confirms the presence of smaller molecules that might result from PLA degradation.

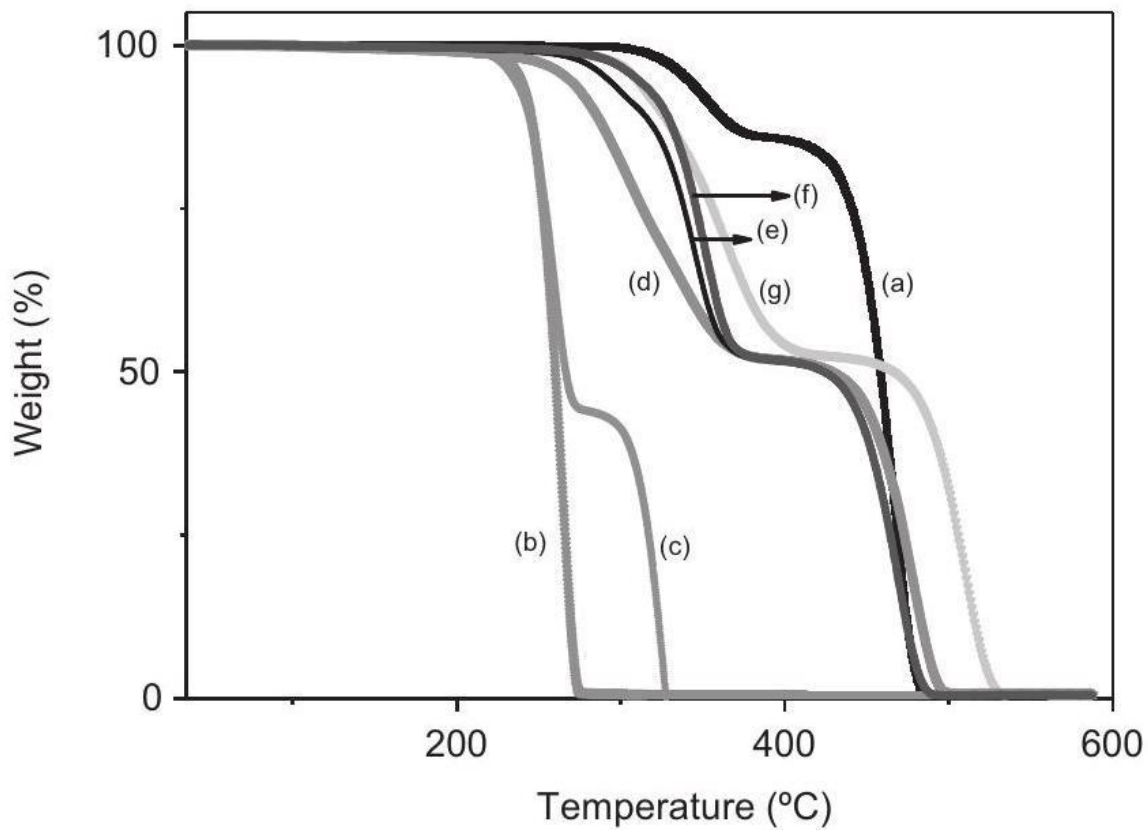


Fig. 5. Thermograms of (a) EVA, (b) PLA, (c) EVAPLA0, (d) EVAPLA1 (e) EVAPLA2, (f) EVAPLA3 and (g) EVAPLA4.

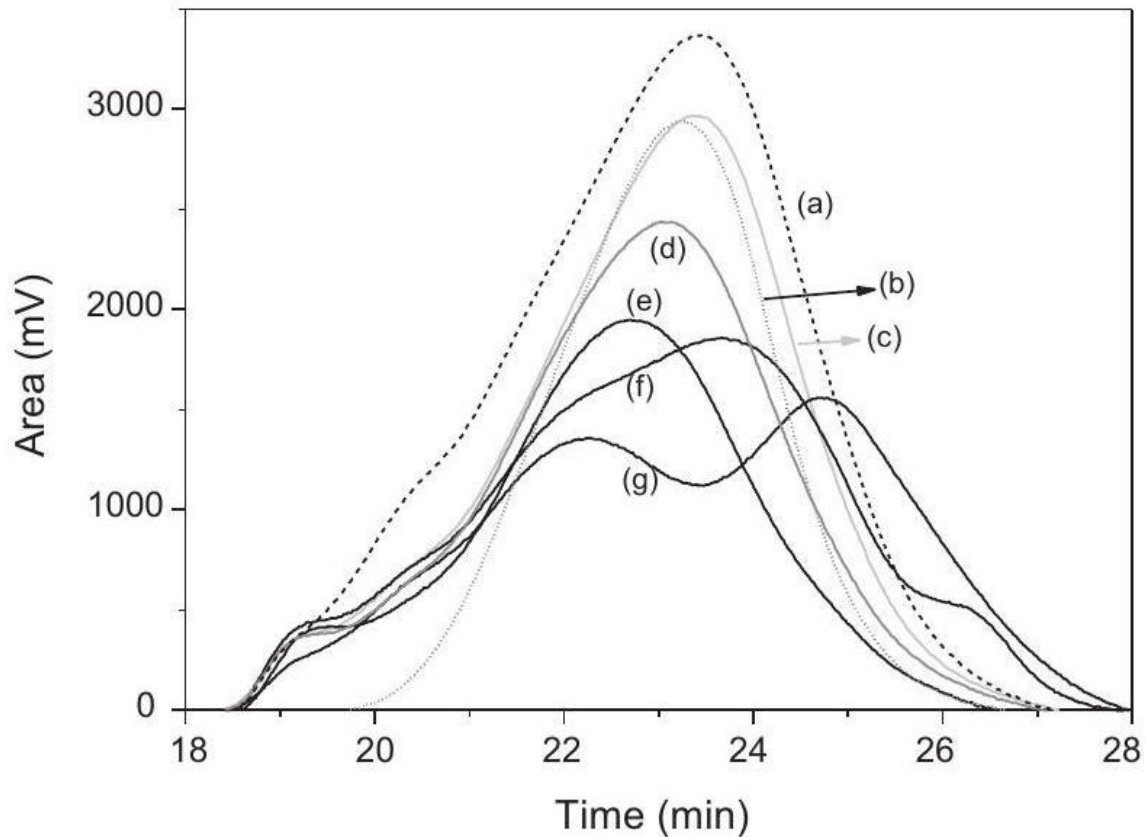


Fig. 6. SEC chromatographs of (a) EVA, (b) PLA, (c) EVAPLA0, (d) EVAPLA1, (e) EVAPLA2, (f) EVAPLA3 and (g) EVAPLA4.

Morphology and properties

Fig. 7 depicts the morphology of the samples analysed by SEM after fracture in liquid nitrogen. The morphology of all prepared samples consists in dispersed PLA particles in the EVA matrix, but significant differences can be observed among them. While sample EVA/PLAO (Fig. 7a) exhibits a coarse morphology, the PLA particles are almost undetectable in EVA matrix of sample EVAPLA4 (Fig. 7b). This change in morphology can be explained by the copolymer formation during reaction, which acts as compatibilizer decreasing the interfacial tension between blend components and consequently the size of the dispersed phase.

Tables 4 and 5 present the melting temperature and crystallinity degree obtained from DSC measurements of neat polymers and prepared samples. The melting temperature and the crystallinity degree of EVA and PLA of the physical blend is practically the same as the values obtained for individual components. Due to the immiscibility between EVA and PLA, it would be expected that both polymers kept their thermal properties.

The results of EVAPLA1 and EVAPLA2 present small changes in melting temperature and crystallinity degree when compared to individual blend components or physical blend, which can be

Table 4
Melting temperature (T_m , °C), melting enthalpy (ΔH , Jg⁻¹) and crystallinity degree (X_c , %) of neat polymers.

Polymer	T_m (°C)	ΔH (Jg ⁻¹)	ΔH° (Jg ⁻¹)	X_c (%)
EVA	85.4	11.6	44	26.4
PLA	150.0	25.7	93.6	27.5

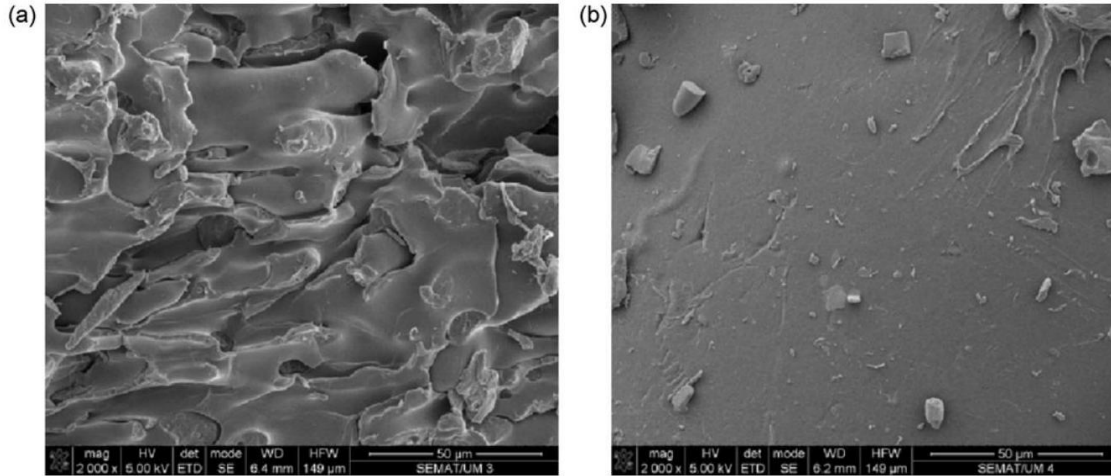


Fig. 7. SEM micrographs of samples (a) EVAPLA0 and (b) EVAPLA4.

Table 5
Melting temperatures (T_m , °C), melting enthalpy (ΔH , Jg⁻¹), and crystallinity degree (X_c , %) of prepared samples.

Sample	EVA			PLA		
	T_m (°C)	ΔH (Jg ⁻¹)	X_c (%)	T_m (°C)	ΔH (Jg ⁻¹)	X_c (%)
EVAPLA0	86.7	8.8	20.0	149.0	23.2	24.8
EVAPLA1	86.0	8.3	18.9	143.5	24.6	26.2
EVAPLA2	85.7	8.2	18.6	143.3	23.8	25.4
EVAPLA3	85.2	7.7	17.5	141.3	22.8	24.3
EVAPLA4	85.0	7.5	17.0	140.2	20.2	21.5

due to small PLA amount in EVA domains. However, EVAPLA4 presents considerable change in the melting temperature of PLA, from 150.0°C to 140.2°C, but the melting temperature of EVA is very similar to the initial EVA. Moreover, the crystallinity degree decreased for both polymers. This difference could be related with the increase in compatibility between EVA and PLA, as observed by SEM.

The decrease of crystallinity degree, namely for EVAPLA3 and EVAPLA4 is related to the transesterification reactions and its extent, from which result covalent bonds between PLA and EVA segments leading to a lower regularity of the molecular structure. Also, the occurrence of transesterification reactions leads to changes of molecular structures of the polyesters, which promotes changes of crystallinity.

Elongation at break and Young modulus as a function of copolymer amount are depicted in Fig. 8. The addition of PLA ($\epsilon = 8.0\%$) to EVA ($\epsilon = 329.2\%$) resulted in lower flexible materials, i.e., a decrease of the elongation at break was observed, namely for physical blends, where the copolymer amount was zero. This result can be explained

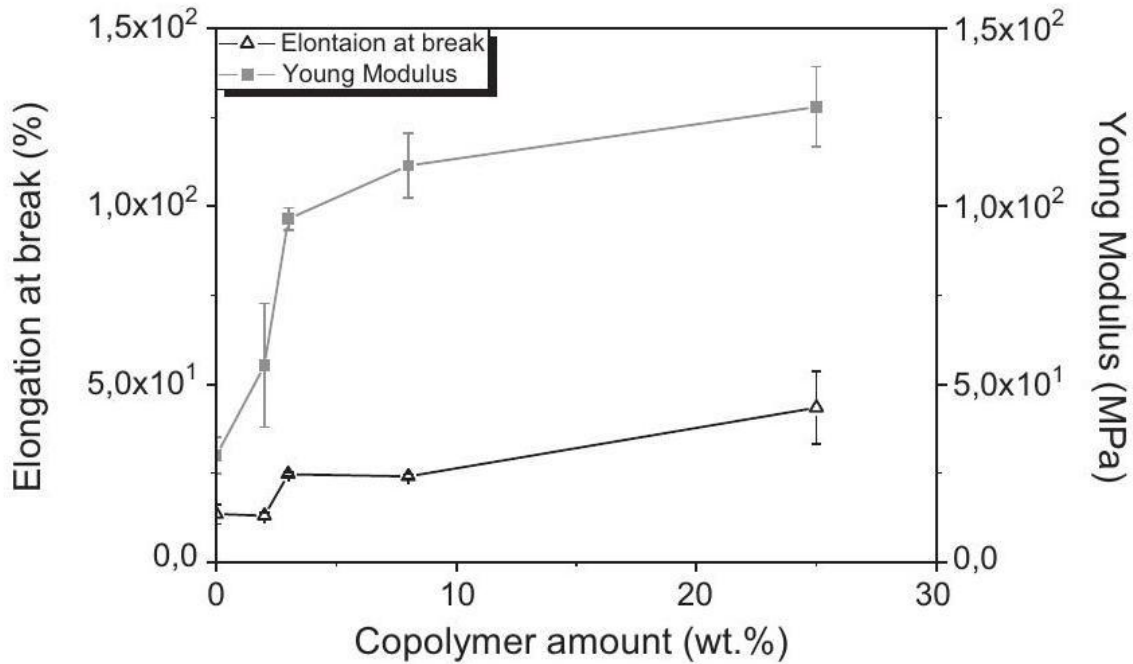


Fig. 8. Young modulus and elongation at break as function of copolymer amount.

Table
Elemental analysis of all samples.

Sample	Carbon (%)	Hydrogen (%)	Oxygen (%)	Chemical formula
EVAPLA0	66.7	9.5	23.9	C ₄ H ₆ O
EVAPLA1	67.5	9.7	22.7	C ₄ H ₇ O
EVAPLA2	67.6	9.7	22.7	C ₄ H ₇ O
EVAPLA3	68.3	10.0	21.7	C ₄ H ₇ O
EVAPLA4	69.1	10.0	20.9	C ₄ H ₈ O

by the immiscibility of the blend components. Nevertheless, as the copolymer amount increased the elongation at break increased. A similar trend was observed for Young

modulus (Fig. 8), blending EVA (19 MPa) and PLA (450 MPa) decreased the value of PLA Young modulus. However, it became greater for higher copolymer amounts.

This enhancement can be attributed to the formation of EVA-g-PLA copolymer and its compatibility effect, as observed by SEM (Fig. 7).

Biodegradability

The biodegradability of the prepared samples was characterized by biochemical oxygen demand, where biodegradability is expressed as the amount of O_2 consumed during biodegradation divided by their theoretical oxygen demand (ThOD), using the elemental analysis data of Table 6. The values of the theoretical

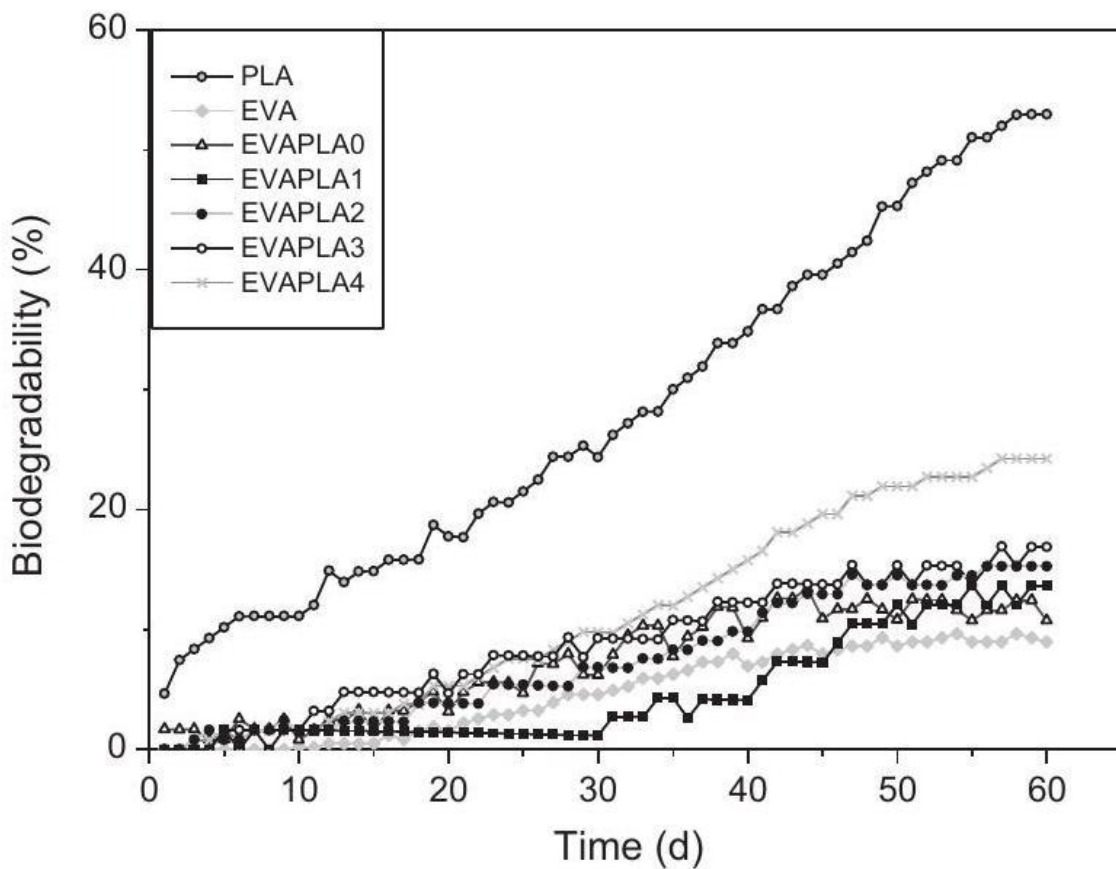


Fig. 9. Percentage of biodegradation of the copolymers and blend according to ISO 14851 (1999).

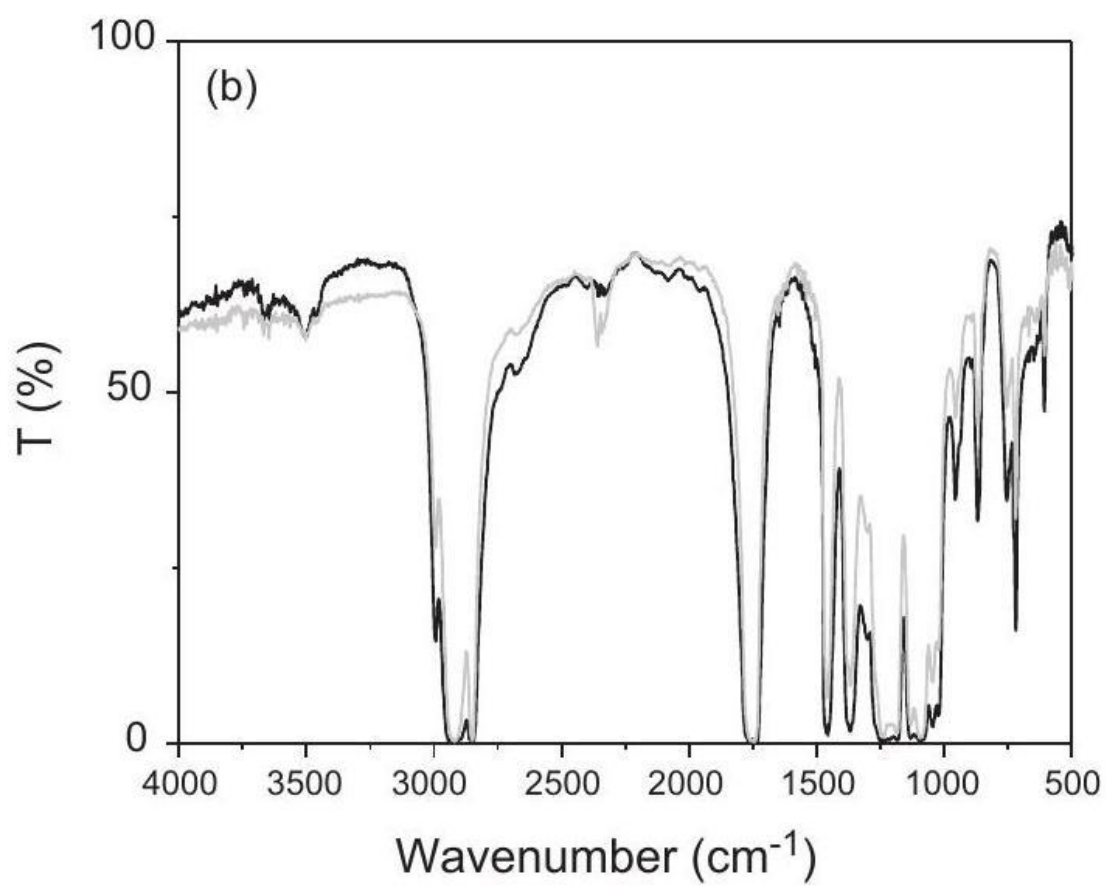
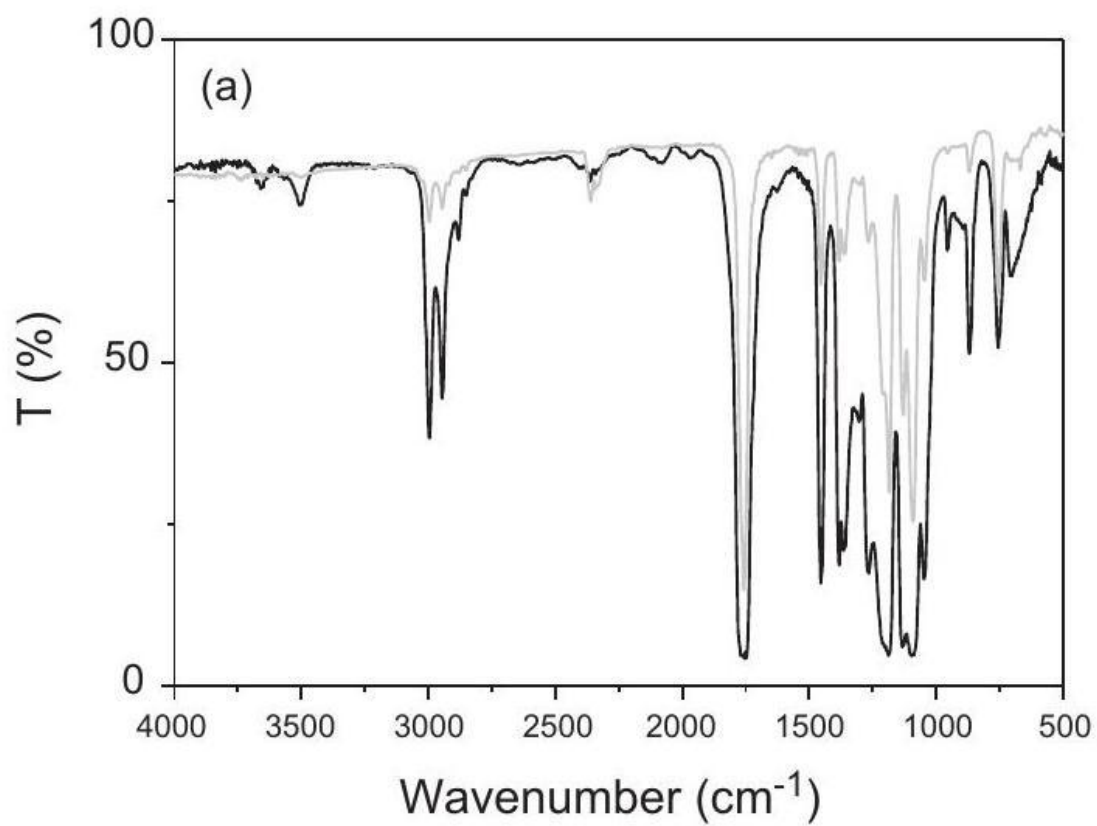


Fig. 10. FTIR spectra of undegraded (black line) and biodegraded (gray line) blends: (a) PLA, (b) EVAPLA0 and (c) EVAPLA4. oxygen demand were calculated based on elemental analysis of each sample. The results during 60 days of biodegradation are presented in Fig. 9. Among the neat polymers, EVA shows the lowest degree of biodegradability and PLA the highest. This would be expected because it is well known that aliphatic polyesters are biodegradable in a wide variety of ecosystems [18]. Several studies performed to evaluate the biodegradability of PLA indicated that PLA films were more biodegradable under composting conditions at higher temperatures (58°C), 55% [19], 64% [20], and 86% [21], than at lower temperatures (30°C), 3.7% [22] in the aquatic tests. The fact that higher temperatures favour non-enzymatic hydrolysis of ester bonds support the results obtained for PLA films [23,24]. These values cannot be directly compared with the value obtained in the present study, around 52.9%(30°C), once the molar mass, biodegradability methods, experimental conditions and length of the assays used were different.

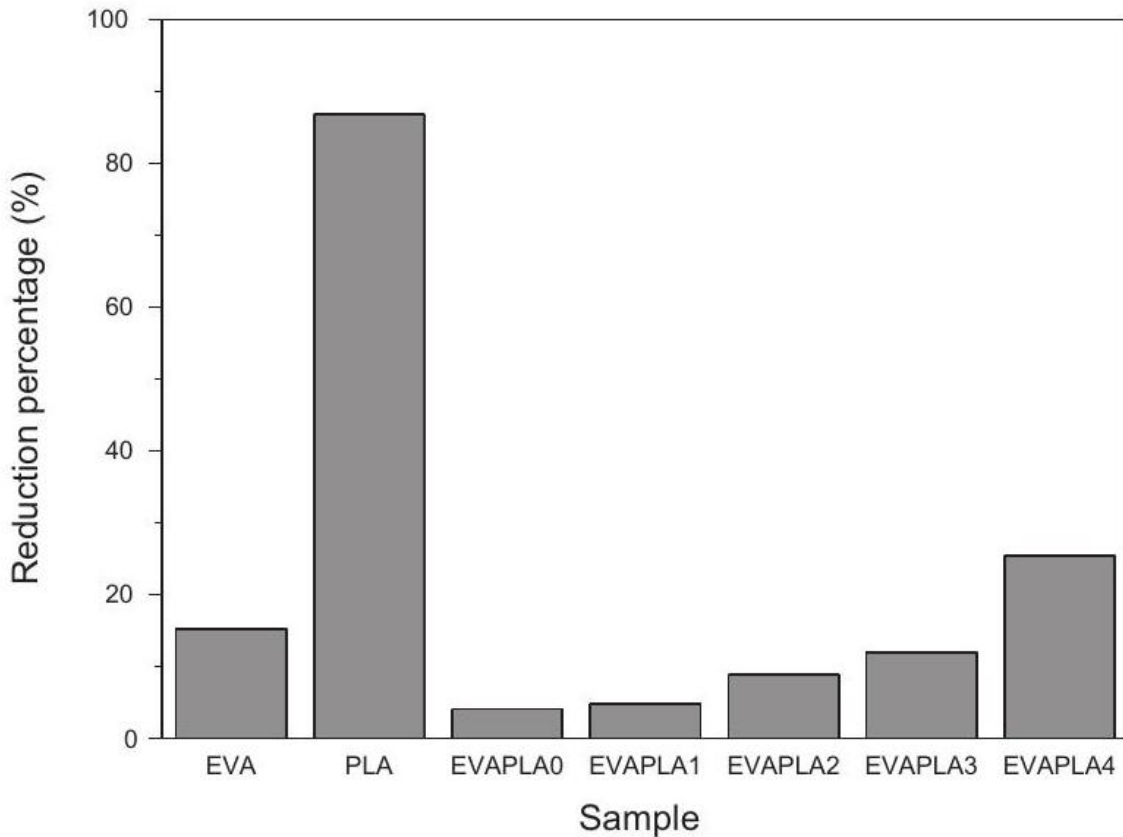


Fig. 11. Reduction percentage molar mass of the samples before and after biodegradation.

Blending PLA with EVA had a positive effect on biodegradability of the latter, as EVAPLA0 (10.7%) exhibited slightly higher biodegradability than EVA (8.9%). Samples containing grafted copolymers showed higher biodegradability, EVAPLA4 exhibited the highest value (24.2%). Literature studies reported that grafting reactions favour the formation of branched/crosslinked structures, promoting the increase of the amorphous zones concentration in the polymer [24]. Furthermore, it seems that the microbial accessibility to ethylene vinyl acetate groups increases when higher amount of PLA are grafted to EVA.

Comparing samples with copolymers to physical blend, it is possible to observe that the crystallinity decreases (see Tables 4 and 5), which is followed by a decrease of the melting temperature. Therefore, the increase in the concentration of amorphous regions increases the biodegradability, because of the higher mobility of the chains and their higher mobility to the microorganisms.

To evaluate the extent of biodegradation of all samples, FTIR spectra of initial and biodegraded samples were recorded (Fig. 10). Each Figure contains two spectra, corresponding to initial and biodegraded material. As expected, in the case of EVA no significant changes occurred (data not shown), because EVA is a non-biodegradable polymer. The major changes occurred for PLA spectrum (Fig. 10a). Concerning PLA, transmittance data on a common scale showed that all peaks decreased after biodegradation. The reduction in the CH-asymmetric and CH-symmetric stretches at 2920 cm^{-1} and 2850 cm^{-1} , respectively, indicated a reduction of the molar mass of the PLA. The decrease of peaks related to carbonyls (1800 cm^{-1} and 1700 cm^{-1}) and ethers (1100 cm^{-1}) indicated chain scission. A reduction of the peak at 1460 cm^{-1} was associated with decrease of CH_3 side groups.

FTIR spectra of EVAPLA0 (Fig. 10b) shows that no major changes occurred during biodegradation. The small differences are probably related to PLA consumption in the physical blend, during the metabolism of microorganisms, resulting in a small reduction of molar mass, since EVA is a non-biodegradable polymer, as previously described. Even though similar results were obtained for EVAPLA4 (Fig. 10c), the decrease in the intensity of all peaks is more pronounced, which is in agreement with the BOD results and confirmed by the reduction in the molar mass of the samples (see Table 3). These results can be explained based on consumption of carbon in the polymer chains by the microorganisms, i.e., presented a significant reduction in the intensity of the peaks corresponding to the groups C – H, C = O, C – O. This reduction might have been due to the metabolism of oxygen consumption microorganisms, as suggested by the BOD test.

The biodegradation was also evaluated, in a quantitative way, by SEC measurements (see Table 3 and Fig. 11). PLA, as expected, suffered the highest molar mass reduction (86.8%). Among all the prepared samples, EVAPLA4, which contains higher copolymer amount, shows the highest decrease in number average molar mass (25.5%). Moreover, the main distribution peak had obviously shifted to the right side (data not shown) confirming the scission of the main chain and consequently oligomers formation. After 60 days of biodegradation the retention time increased and the intensity of peak slightly decreased.

Conclusions

Copolymers of EVA-g-PLA were synthesized using titanium propoxide and titanium phenoxide as catalysts, which were characterized by several analytical techniques.

Changing the ratio of PLA and catalyst resulted in a series of graft copolymers, which allowed to prepare materials with different rheological, thermal and mechanical properties.

Biodegradability results showed that PLA is more biodegradable than EVA based on biochemical oxygen demand. Differences in biodegradability behaviour were observed between the physical blend and the samples containing copolymers. The qualitative and

quantitative, by FTIR and SEC results, showed that EVAPLA4 was the more biodegradable.

The results obtained in this work show that the method employed is a promising route to produce bio-based materials with good mechanical properties, which could be used in technological applications.

Acknowledgements

The authors acknowledge the financial support given by FCT through the project PTDC/AMB/73854/2006 and the PhD grant SFRH/BD/29802/2006.

References

- [1] E.S. Stevens, *Green Plastics: An Introduction to the New Science of Biodegradable Plastics*, Princeton, Princeton University Press, 2002.
- [2] N. Saha, M. Zatloukal, P. Saha, *Polym. Adv. Technol.* 14 (2003) 854-860.
- [3] S.C. Tjong, J.Z. Bei, *Polym. Eng. Sci.* 38 (1998) 392-402.
- [4] L. Yu, K. Dean, L. Li, *Prog. Polym. Sci.* 31 (2006) 576-602.
- [5] A.V. Machado, I. Moura, F.M. Duarte, G. Botelho, R. Nogueira, A.G. Brito, *Int. Polym. Proc.* 21 (2007) 512-518.
- [6] G. Biseraw, C.J. Carriere, *Compos A-Appl. Sci.* 35 (2004) 313-320.
- [7] E.M. Nakamura, L. Cordi, G.S.G. Almeida, N. Duran, L.H.I. Mei, *J. Mater. Process. Technol.* 162-163 (2005) 236-241.
- [8] L. Contat-Rodrigo, A.R. Greus, *J. Appl. Polym. Sci.* 83 (2002) 1683-1691.
- [9] P. Matzinos, V. Tserki, C. Gianikouris, E. Pavlidou, C. Panayiotou, *J. Eur. Polym.* 38 (2002) 1713-1720.
- [10] M. Mochizuki, K. Mukai, K. Yamada, N. Ichise, S. Murase, Y. Iwaya, *Macromolecules* 30 (1997) 7403-7407.
- [11] W. Baker, C. Scott, H. Hug, *Reactive Polymer Blending*, Hanser Publishers, Connecticut, 2001.
- [12] I. Moura, A.V. Machado, R. Nogueira, V. Bounor-Legare, *React. Funct. Polym.* 71 (2011) 694-703.
- [13] J. Cayuela, V. Bounor-Legaré, P. Cassagnau, A. Michel, *Macromolecules* 39 (2006) 1338-1346.
- [14] ISO 14851. Determination of the ultimate aerobic biodegradability of plastic materials in an aqueous medium-method by measuring the oxygen demand in a closed respirometer, 1999 (Withdrawn 2005).
- [15] W. Bahloul, V. Bounor-Legaré, F. Fenouillot, P. Cassagnau, *Polymer* 50 (2009) 2527-2534.
- [16] L. Zhang, W. Xie, X. Zhao, Y. Liu, W. Gao, *Thermochim. Acta* 495 (2009) 57-62.
- [17] N.S. Allen, M. Edge, M. Rodriguez, C.M. Liauw, E. Fontan, *Polym. Degrad. Stab.* 68 (2000) 363-371.
- [18] T. Fujimaki, *Polym. Degrad. Stab.* 59 (1998) 209-214.
- [19] R. Iovino, R. Zullo, M.A. Rao, L. Cassar, L. Gianfreda, *Polym. Degrad. Stab.* 93 (2008) 147-157.
- [20] T. Kijchavengkul, R. Auras, M. Rubino, M. Ngouajio, R. Fernandez, *Polym. Test.* 25 (2006) 1006-1016.
- [21] G. Kale, R. Auras, S. Singh, R. Narayan, *Polym. Test.* 26 (2007) 1049-1061.
- [22] V. Massardier-Nageotte, C. Pestre, T. Cruard-Pradet, R. Bayard, *Polym. Degrad. Stab.*

- 91 (2006) 620-627.
[23] A.M. Reed, D.K. Gilding, Polymer 22 (1981) 494-498.
[24] N.T. Lotto, M.R. Calil, C.G.F. Guedes, D.S. Rosa, Mater. Sci. Eng. C-Biol. Sci. 24 (2004) 659-662.

E-mail addresses: isabelm@dep.uminho.pt (I. Moura), regina@deb.uminho.pt (R. Nogueira), bounor@univ-lyon1.fr (V. Bounor-Legare), avm@dep.uminho.pt (A.V. Machado).